further with T. This degree of disorder gives, on average, at least two nearest neighbors occupying a misoriented configuration. Our results are consistent with this model. Any fraction of orientationally disordered C_{60} molecules greater than 1/12 would be sufficient to induce a dipole on essentially all molecules. Recent calculations (*4*) have shown that this rotation about a threefold axis should be separated by a 300-meV barrier, which is also consistent with our results. For completeness, we note that the disorder could also originate at nonorientationally induced crystallographic defects such as domain boundaries, stacking faults, or twins. The crystal would have to be highly defective to have at least 10^{-3} of its molecules at disordered interfaces.

Finally, we can address the question of "glassy" behavior in crystalline C_{60}. Our results show a high degree of static orientational disorder and invite a comparison with the well-studied orientational glass $KBr_{1-x}(CN)_x$. The width of the barrier height distribution in $KBr_{0.5}(CN)_{0.5}$ is 30 meV (*20*), quite comparable to the 40-meV width for C_{60}. But in $KBr_{0.5}(CN)_{0.5}$ the mean barrier energy E_0 is 60 meV such that the fractional width is $W/E_0 \approx 0.5$, whereas in C_{60} the mean barrier energy is 270 meV and the fractional width is $W/E_0 \approx 0.15$. Therefore, if the fractional width is generated by intermolecular interactions, then they must be less important in C_{60} relative to glassy $KBr_{0.5}(CN)_{0.5}$. We also note that $KBr_{1-x}(CN)_x$ has no glassy phase for $x > 0.7$ where $W/E_0 < 0.4$ (*20*). Another signature of glassy behavior would be deviations from Arrhenius behavior resulting in a Vogel-Fulcher law near a glass transition. Figure 3 shows no deviations from Arrhenius behavior for the temperature range $130\ K < T < 190\ K$. In addition, thermal conductivity measurements (*12*), which extended to 85 K, have found $E_0 = 240 \pm 30$ meV, close to our higher temperature results. The consistency of these different measurements over a large spread in time scales would imply that Arrhenius behavior persists to 85 K (*24*). Therefore, whether C_{60} has quenched disorder or a low-temperature glassy phase appears to be an open question for the moment.

Our results indicate that cubic crystals of solid C_{60} couple to low-frequency electric fields in a way that reflects the orientational dynamics of the C_{60} molecules. There appears to be a relatively large amount of structural disorder, most likely originating in the imperfect orientational alignment of adjacent molecules. The disorder creates a distribution of potential barriers for molecular reorientation and breaks the local symmetry sufficiently to allow a permanent electric dipole to exist on a C_{60} molecule.

REFERENCES AND NOTES

1. H. W. Kroto, J. R. Heath, S. C. O'Brien, R. F. Curl, R. E. Smalley, *Nature* **318**, 162 (1985).
2. W. Kratschmer, L. D. Lamb, K. Fostiropoulos, D. R. Huffman, *ibid.* **347**, 354 (1990).
3. P. A. Heiney *et al.*, *Phys. Rev. Lett.* **66**, 2911 (1991); R. Sachidanandam and A. B. Harris, *ibid.* **67**, 1467 (1991).
4. J. P. Lu, X.-P. Li, R. Martin, *ibid.* **68**, 1551 (1992).
5. O. Gunnarsson, S. Satpathy, O. Jepsen, O. K. Andersen, *ibid.* **67**, 3002 (1991).
6. R. Tycko *et al.*, *ibid.*, p. 1886.
7. D. A. Neumann *et al.*, *ibid.*, p. 3808.
8. R. D. Johnson, C. S. Yannoni, H. C. Dorn, J. R. Salem, D. S. Bethune, *Science* **255**, 1235 (1992).
9. W. I. F. David *et al.*, *Nature* **353**, 147 (1991).
10. X. D. Shi *et al.*, *Phys. Rev. Lett.* **68**, 827 (1992).
11. W. I. F. David *et al.*, *Europhysics Lett.* **18**, 219 (1992).
12. R. C. Yu, N. Tea, M. B. Salamon, D. Lorents, R. Malhotra, *Phys. Rev. Lett.* **68**, 2050 (1992).
13. W. P. Beyermann *et al.*, *ibid.*, p. 2046.
14. M. P. Gelfand and J. P. Lu, *ibid.*, p. 1050.
15. Toluene was used in the extraction from the soot, and C_{60} was separated by column chromatography. Sample purity was verified by high-performance liquid chromatography, which found no trace of other fullerenes at a level of a fraction of a percent. The C_{60} powder was then loaded in a quartz tube sealed in a vacuum (10^{-6} torr) and the end of the tube heated to 600°C. High-quality single crystals grew at 350° to 300°C over a period of a few weeks. See R. M. Fleming *et al.*, *Mater. Res. Soc. Symp. Proc.* **206**, 691 (1991).
16. A. F. Hebard, R. C. Haddon, R. M. Fleming, A. R. Kortan, *Appl. Phys. Lett.* **59**, 2109 (1991).
17. Y. Saito *et al.*, *Chem. Phys. Lett.* **189**, 236 (1992).
18. S. Saito and A. Oshiyama, *Phys. Rev. Lett.* **66**, 2637 (1991); W. Y. Ching *et al.*, *ibid.* **67**, 2045 (1991).
19. P. A. Heiney *et al.*, *Phys. Rev. B* **45**, 4544 (1992).
20. R. M. Ernst *et al.*, *ibid.* **38**, 6246 (1988); F. Luty and J. Ortiz-Lopez, *Phys. Rev. Lett.* **50**, 1289 (1983).
21. Uncertainties in the background make a quantitative discrimination among different relaxation functions difficult. For example, a stretched exponential relaxation function yielded a reasonable description of the data.
22. The same Pa3 symmetry of C_{60} is also found in solid H_2 and N_2 with no permanent dipole moment. Intermolecular interactions between quadrupolar H_2 and N_2 can induce a dipolar response for certain phonon modes. See O. Schnepp, *J. Chem. Phys.* **46**, 3983 (1967); J. Van Kranendonk, *Solid Hydrogen* (Plenum, New York, 1983), pp. 114–128.
23. T. Suzuki, Q. Li, K. C. Khemani, F. Wudl, O. Almarsson, *Science* **254**, 1186 (1991).
24. In $KBr_{0.5}(CN)_{0.5}$, a transition to a quadrupolar glass phase occurs near 80 K followed by electric dipolar freezing near 50 K. No anomalies in the dielectric response have been seen at the quadrupolar glass transition. In C_{60}, it is possible that there is an order parameter to which strain and electric field do not couple.
25. We acknowledge helpful conversations with N. O. Birge, S. D. Mahanti, and M. F. Thorpe.

28 April 1992; accepted 28 May 1992

High-Pressure Brillouin Studies and Elastic Properties of Single-Crystal H_2S Grown in a Diamond Cell

H. Shimizu and S. Sasaki

High-pressure Brillouin spectra of crystalline hydrogen sulfide (H_2S) have been measured at up to 7 gigapascals at room temperature. The best fit of the angular dependence of Brillouin acoustic velocities between experimental values and calculations based on Every's expression for elastic waves of an arbitrary direction yielded the orientation of an H_2S cubic crystal grown in the diamond-anvil high-pressure cell. In situ determinations of sound velocities, as a function of pressure, could be made for any direction, the refractive index, the density, and the elastic constants. This method provides a means for the systematic study of elastic properties and phase transitions of condensed gases under ultrahigh pressures.

High-pressure Brillouin scattering is an ideal probe for measuring the sound velocity (v), the refractive index (n) and the elastic constant (C_{ij}) as a function of pressure, and the equation of state (EOS) (*1–4*). When a typical diamond-anvil high-pressure cell (DAC) is used, the probed direction for the wave vector (**q**) of the acoustic phonon propagating in a crystal is considerably limited (*1, 4, 5*): only one or two directions of **q** parallel to the diamond culet faces for a scattering geometry of 90° and only one direction of **q** perpendicular to the diamond faces for the backscattering geometry can be used (*1, 4, 6–8*). It is then necessary to determine accurately the axis orientation of the grown crystal, because the sound velocity is sensitively dependent on the direction of **q** for the probed acoustic phonon, but this has been difficult. Lee *et al.* (*7*) overcame the above problem by the additional use of x-ray diffraction measurements. They determined the axis orientation of a single crystal of orthorhombic hydrogen-bonded HF and measured the high-pressure Brillouin spectra of oriented HF crystals at the near-forward scattering geometry, which yielded the sound velocities as a function of pressure, and the values of five elastic constants divided by the density (C_{ij}/ρ) at a pressure of 2.54 GPa.

Department of Electronics, Gifu University, 1-1 Yanagido, Gifu 501-11, Japan.

For pressure-induced crystalline H_2 and D_2 at pressures above 5.7 GPa and temperatures of 300 K, Shimizu *et al.* (1, 5) measured Brillouin acoustic velocities at scattering geometries of 60°, 90°, and 120° by using the DAC with eight ports for transmitted and scattered light (3). These results showed that crystalline H_2 and D_2 had elastic isotropy under the assumption of homogeneous *n*, which made it easier to determine the EOS. Recent studies (9–11) revealed that the earlier results (1) for *n* as a function of pressure are in good agreement with those determined by the optical interference method (9), but the EOS determined from Brillouin scattering (1) is somewhat softer than that determined directly by the synchrotron x-ray diffraction measurement (10). This discrepancy in the EOS is probably due to the rough estimation for the elastic isotropy of crystalline H_2 and D_2 (1, 5).

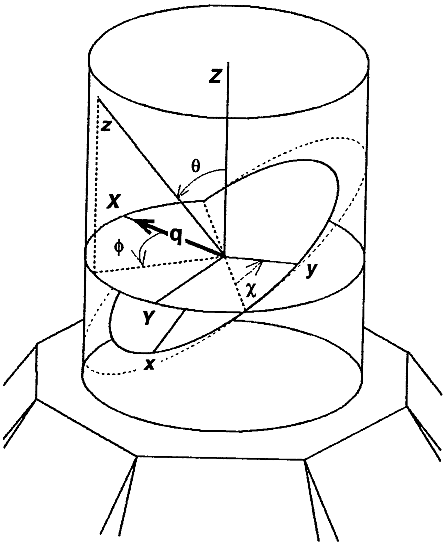

Fig. 1. Euler angles (θ, φ, χ) relating the crystal reference frame (*x, y, z*) and the laboratory frame (*X, Y, Z*). The wave vector **q** of probed acoustic phonons lies in the *XY* plane (90° scattering geometry), which is parallel to the diamond culet face. The load axis corresponds to the central *Z* axis.

For pressure-induced crystalline NH_3 at pressures above 1.2 GPa and temperatures of 300 K, Gauthier *et al.* (8) measured the Brillouin spectra at a scattering geometry of 180° [see equation 2 in (8)] and determined the pressure dependence of *nv* up to 20 GPa. They found that each run yielded a significantly different result. This behavior means that the single crystal grows every time with the different orientation relative to the cell axis. Therefore, it was not easy to determine exactly the elastic properties of crystalline NH_3 (8).

In this report, we demonstrate that the sound velocity, the refractive index, elastic constants, and the EOS of an H_2S single crystal grown in the DAC can be exactly determined by Brillouin scattering measurements with in situ identification of the crystal orientation at each pressure by analyzing the observed angular dependence of Brillouin acoustic velocities.

Hydrogen sulfide (H_2S) is a simple material that forms a hydrogen-bonded network and shows a plastic phase, that is, an orientationally disordered (OD) face-centered cubic (fcc) phase (12). Recent studies of the high-pressure Raman scattering in solid H_2S have shown that there is a pressure-induced phase transition near 11 GPa from OD phase I to a new solid phase IV (13). Therefore, at room temperature the plastic fcc phase is stable from 0.47 to 11 GPa. We condensed commercial gaseous H_2S by spraying its vapor into the gasket hole of the DAC cooled in liquid nitrogen (14). When the hole was full of solidified H_2S, the upper diamond was translated to seal the sample. After adequate pressure had been applied, the DAC was warmed to 300 K. A single crystal was grown by increasing the pressure on a seed crystal, which coexists with the liquid at 0.47 GPa. The pressure was measured by the ruby-scale method.

For Brillouin measurements, the 488.0-nm argon-ion laser line (λ_0) with a single longitudinal mode was used at input power levels from 100 to 300 mW. The heart of the apparatus was a plane piezoelectrically scanned Fabry-Perot interferometer (Burleigh DAS-10), which was used in a five-pass configuration. The 90° Brillouin scattering geometry was used principally to determine the sound velocity (v_{90}). The Brillouin frequency shift ($\Delta\nu_{90}$) is related to v_{90} by the expression

$$v_{90} = \Delta\nu_{90} \cdot \frac{\lambda_0}{\sqrt{2}} \qquad (1)$$

which is independent of the refractive index of the medium (15). The crystallographic axes of a single crystal grown in the DAC are usually determined by x-ray diffraction. We instead identified the crystal orientation by using only the Brillouin scattering, accompanied by an in situ determination of the elastic properties under each applied pressure. The crystal reference frame (*x, y, z*) is related to the laboratory frame (*X, Y, Z*) by the use of the Euler angles (θ, φ, χ) (Fig. 1). In order to determine the Euler angles and elastic properties of solid H_2S in the DAC, we developed a DAC having symmetric conical

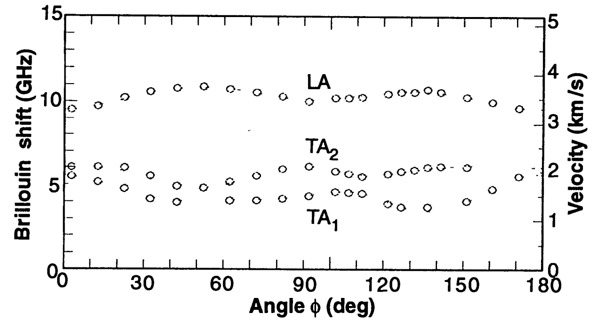

Fig. 2. Brillouin frequency shifts and sound velocities of LA, TA_1, and TA_2 modes as a function of angle φ at a scattering geometry of 90° and *P* = 1.50 GPa in the fcc plastic phase of crystalline H_2S. Open circles indicate experimental points, and the dotted lines represent the calculated best fit velocities.

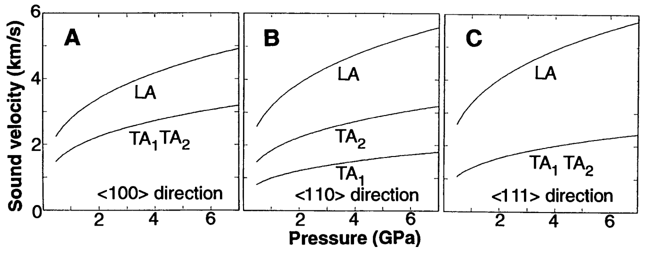

Fig. 3. The pressure dependence of sound velocities calculated by the use of Euler angles for (**A**) <100>, (**B**) <110>, and (**C**) <111> directions in the fcc plastic phase of crystalline H_2S.

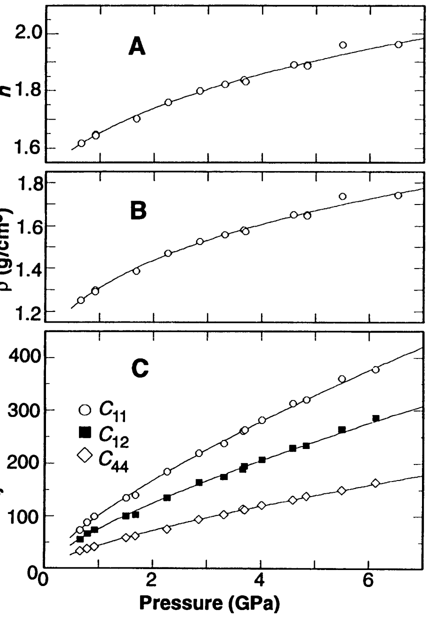

Fig. 4. The pressure dependences of (**A**) the refractive index *n*, (**B**) the density ρ, and (**C**) elastic constants C_{11}, C_{12}, and C_{44} in the fcc plastic phase of crystalline H_2S.

openings with aperture angles of 98°. This geometry allows us to probe acoustic phonons propagating in any direction parallel to diamond faces. Brillouin measurements at a scattering geometry of 90° (angle accuracy, 0.5°) were made in 10° intervals of rotation angle ϕ in the laboratory frame, namely, the rotation of DAC about the load axis with an uncertainty of ±0.2°. The observed Brillouin frequency shifts, that is, sound velocities at 1.50 GPa, are plotted as a function of ϕ as open circles in Fig. 2.

To analyze the angular dependence of acoustic velocities of the longitudinal (LA) and two transverse, slow (TA_1) and fast (TA_2), modes at each applied pressure, it is necessary to use the usual Brillouin equation and Every's closed-form expressions (*16*) relating sound velocities for arbitrary directions to the elastic constants. We can easily modify Every's velocity expressions for cubic crystals to our experimental system by using the Euler angles, instead of the direction cosines of **q** in the crystal axis frame. The velocities can therefore be expressed as a function of six parameters: $v_i^2 = f(C_{11}/\rho, C_{12}/\rho, C_{44}/\rho, \theta, \phi, \chi)$, where the subscript i indicates LA, TA_1, and TA_2 modes. A computerized least-squares fit was applied to determine elastic properties of the fcc H_2S crystal at each pressure. There is excellent agreement between the measured and the fitted values, because each elastic constant depends anisotropically or dominantly on its special directions. The best fitting results yielded $C_{11}/\rho = 98.0$, $C_{12}/\rho = 72.9$, and $C_{44}/\rho = 43.4$ kbar · cm³/g at 1.50 GPa. An independent procedure for different crystal orientations showed excellent consistency for these values within an accuracy of ±2%.

The pressure dependences of the crystal orientation and elastic properties were determined by the best fit to the angular dependence of sound velocities under each applied pressure. The single crystal orientation changed in the DAC by the increasing uniaxial stress component with pressure: (θ, ϕ, χ); (76.4; 6.8, 21.2), (77.0, 7.1, 19.8), and (79.2, 11.0, 17.7) at pressures of 3.69, 4.58, and 6.12 GPa, respectively, where the measurements were made on the same point of the H_2S crystal. These data indicate that it is necessary to make in situ determinations of both the crystal orientation and the elastic properties at each applied pressure in order to study condensed gases in the DAC. From the set of six parameters obtained, the sound velocities could be calculated for all directions of each crystal orientation (see Fig. 3 for typical directions). Furthermore, we can calculate the acoustic velocities (v_{180}) along the Z direction (load axis) in the laboratory frame, which are available to determine n as follows: At backscattering geometry (180°) the Brillouin frequency shift ($\Delta\nu_{180}$) is related to v_{180} by the expression

$$v_{180} = \Delta\nu_{180} \cdot \frac{\lambda_0}{(2n)} \qquad (2)$$

By using the measured $\Delta\nu_{180}$ and the calculated v_{180} by the best fitting method, we could estimate n from Eq. 2 at each applied pressure (Fig. 4A). The value of n is 1.69 at 1.50 GPa and increases with pressure up to 1.98 at 7.0 GPa. From these results, the Lorentz-Lorenz relation $(n^2 - 1)/(n^2 + 2) = 4\ \pi N\rho\alpha/3M$ yields ρ as a function of pressure (Fig. 4B), that is, the EOS, where N is Avogadro's number, M is the molecular weight, and α is polarizability with a value of 3.78×10^{-24} cm³ (*17*), which is assumed to be pressure-insensitive (*18*). The density, ρ, is 1.37 g/cm³ at 1.50 GPa and increases with pressure up to 1.78 g/cm³ at 7.0 GPa (*19*). For the present method, the error is within $\Delta\rho/\rho = \pm 3.8\%$ for $n = 1.7$, where the uncertainties in the measured frequency shift and in the determined refractive index are about $\Delta(\Delta\nu)/\Delta\nu = \pm 1\%$ and $\Delta n/n = \pm 2\%$, respectively.

Finally, on the basis of the pressure dependence of ρ, the elastic constants C_{11}, C_{12}, and C_{44} were determined as a function of pressure (Fig. 4C). The elastic anisotropy $A = 2C_{44}/(C_{11} - C_{12})$ is calculated to be 3.45 at 1.50 GPa. This is close to the value of 3.60 for fcc plastic crystal CH_4 at 1 bar and 90 K (*20*).

High-pressure Brillouin spectroscopy provides a new approach for the study of elastic properties of condensed gases in the DAC under ultrahigh pressures. It will be worthwhile to apply this new method to the fcc and hexagonal close-packed systems for simple condensed gases under ultrahigh pressures.

REFERENCES AND NOTES

1. H. Shimizu, E. M. Brody, H. K. Mao, P. M. Bell, *Phys. Rev. Lett.* **47**, 128 (1981).
2. A. Jayaraman, *Rev. Mod. Phys.* **55**, 65 (1983).
3. R. J. Hemley, P. M. Bell, H. K. Mao, *Science* **237**, 605 (1987).
4. M. Grimsditch and A. Polian, in *Simple Molecular Systems at Very High Density*, A. Polian, P. Loubeyre, N. Boccara, Eds. (Plenum, New York, 1989), pp. 237–255.
5. H. Shimizu, T. Kumazawa, E. M. Brody, H. K. Mao, P. M. Bell, *Jpn. J. Appl. Phys.* **22**, 52 (1983).
6. A. Polian and M. Grimsditch, *Phys. Rev. Lett.* **52**, 1312 (1984).
7. S. A. Lee, D. A. Pinnick, S. M. Lindsay, R. C. Hanson, *Phys. Rev. B* **34**, 2799 (1986).
8. M. Gauthier, Ph. Pruzan, J. C. Chervin, A. Polian, *Solid State Commun.* **68**, 149 (1988).
9. J. van Straaten and I. F. Silvera, *Phys. Rev. B* **37**, 1989 (1988).
10. H. K. Mao *et al.*, *Science* **239**, 1131 (1988).
11. R. J. Hemley *et al.*, *Phys. Rev. B* **42**, 6458 (1990).
12. E. Sandor and S. O. Ogunade, *Nature* **224**, 905 (1969).
13. H. Shimizu, Y. Nakamichi, S. Sasaki, *J. Chem. Phys.* **95**, 2036 (1991).
14. ______, in *Molecular Systems Under High Pressure*, R. Pucci and G. Piccitto, Eds. (Elsevier, Amsterdam, 1991), pp. 273–281.
15. C. H. Whitfield, E. M. Brody, W. A. Bassett, *Rev. Sci. Instrum.* **47**, 942 (1976).
16. A. G. Every, *Phys. Rev. Lett.* **42**, 1065 (1979).
17. J. O. Hirschfelder, C. F. Curtiss, R. B. Bird, *Molecular Theory of Gases and Liquids* (Wiley, New York, 1963).
18. Because H_2S molecules exist in a nearly homogeneous field of the plastic (OD) phase, this assumption is reasonable.
19. The thermodynamic relation,

$$\rho(P_B) - \rho(P_A) = \int_{P_A}^{P_B} (\gamma_s/v_s^2)\,dP$$

where P is pressure, also gives us an estimate of the EOS (*1–4*), where $\gamma_s = C_P/C_V$ is the ratio of the specific heats at constant pressure to constant volume, and $v_s^2 = (C_{11}/\rho + 2C_{12}/\rho)/3$ for the cubic system. By using the present EOS determined from the Lorentz-Lorenz relation and the pressure dependence of v_s^2, we could estimate the reasonable pressure dependence of γ_s; $\gamma_s = 1.1$ at 0.5 GPa and decreases to 1.0 at pressures above 2 GPa.
20. S. C. Rand and B. P. Stoicheff, *Can. J. Phys.* **60**, 287 (1982).

11 February 1992; accepted 7 May 1992

Evidence for Liquid-Phase Cirrus Cloud Formation from Volcanic Aerosols: Climatic Implications

Kenneth Sassen

Supercooled droplets in cirrus uncinus cell heads between −40° and −50°C are identified from Project FIRE [First ISCCP (International Satellite Cloud Climatology Project) Regional Experiment] polarization lidar measurements. Although short-lived, complexes of these small liquid cells seem to have contributed importantly to the formation of the cirrus. Freezing-point depression effects in solution droplets, apparently resulting from relatively large cloud condensation nuclei of volcanic origin, can be used to explain this rare phenomenon. An unrecognized volcano–cirrus cloud climate feedback mechanism is implied by these findings.

Pilots and scientist observers have reported that aircraft icing is occasionally observed while flying through high-altitude cirrus clouds at temperatures colder than −40°C. Such reports fly in the face of conventional wisdom, however, because airframe icing under such conditions implies the accretion of liquid cloud droplets supercooled to tem-

Department of Meteorology, University of Utah, Salt Lake City, UT 84112.